Time-Resolved UV-IR Experiments Suggest Fe-Cu Dinuclear Arene Borylation Catalyst Can Be Photoactivated

Jacob T. Davis, Erin E. Martinez, Kyle J. Clark, Doo-Hyun Kwon, Michael R. Talley, David J. Michaelis, Daniel H. Ess,* and Matthew C. Asplund**

Department of Chemistry and Biochemistry, Brigham Young University, Provo, Utah 84602 USA

ABSTRACT

Heterodinuclear complexes with a direct metal-metal bond offer the possibility of unique mechanisms and intermediates. The $Cp(CO)_2Fe$-Cu(IPr) (IPr = N,N-bis(2,6-diisopropylphenyl)imidazol-2-ylidene) heterodinuclear complex **1** was reported to photochemically catalyze arene borylation. To examine possible initial steps of photo-initiated catalysis, we synthesized a triethylsilyl-substituted Fe-Cu catalyst **5** that provided cyclohexane solubility to conduct time-resolved UV-IR studies. Time-resolved vibrational spectroscopic measurements suggest that photolysis of **5** stimulates CO dissociation without Fe-Cu metal-metal bond cleavage. UV-IR measurements of **5** with added pinacolborane (HBPin) showed a very similar set of IR bleaches and a new monocarbonyl IR absorbance, and HBPin appears to stabilize the monocarbonyl species. This suggests that arene borylation catalysis may begin with a photochemical step rather than a relatively endothermic cleavage of the Fe-Cu bond and therefore a new possible catalytic cycle is proposed.

INTRODUCTION

Compared to catalysts with a single metal and ligand framework, transition-metal heterodinuclear catalysts with a direct metal-metal bond offer the potential of unique mechanisms and intermediates, oxidation states, reactivity, and selectivity, especially for bond activation reactions.[1] One way dinuclear catalysts induce unique mechanisms and reactivity is through activation of substrates across two metal centers (e.g. dinuclear oxidative addition, Scheme 1a). While heterodinuclear-mediated and catalyzed reactions were reported for classic transformations, such as alkene and ketone hydrogenation,[2] α-olefin hydroformylation,[3] ethylene polymerization,[4] and olefin metathesis,[5] recently there has been a large effort to exploit dinuclear catalysts for very challenging transformations.[6,7,8,9,10] However, a major limitation to the further design and use of heterodinuclear catalysts is the identification of catalytic intermediates and mechanisms. In many heterodinuclear-catalyzed reactions the mechanism responsible for unique reactivity and/or selectivity is unknown.

Mankad recently reported the photochemical catalytic arene borylation using the $Cp(CO)_2Fe$-Cu(IPr) heterodinuclear complex **1** (Scheme 1b; (IPr = N,N-bis(2,6-diisopropylphenyl)imidazol-2-ylidene)).[11] In this reaction with yields up to 70%, the B-H bond of pinacolborane (HBpin) and the C-H bond of arenes are activated and coupled, which for benzene results in phenylboronoic acid pinacol ester (PhBpin). Based on earlier work from Hartwig,[12] the original mechanistic proposal involved thermal HBpin bond activation to generate the pair of mononuclear species (IPr)Cu-H and $Cp(CO)_2Fe$-BPin (Scheme 1c). Then, photo-promoted CO ejection leads to the mononuclear, coordinately unsaturated Cp(CO)Fe-BPin intermediate that reacts with benzene to produce PhBpin. A ligand crossover experiment was performed as evidence of thermal/dark reactions for ligand exchange with complex **1**. For example, mixing

(IPr)CuFeCp*$(CO)_2$ with (IMes)CuFeCp$(CO)_2$ (IMes = N,N'-bis(2,4,6-trimethylphenyl)imidazol-2-ylidene) results in (IPr)CuFeCp$(CO)_2$ and (IMes)CuFeCp*$(CO)_2$. However, this thermal crossover reaction required 48 hours to reach equilibrium and based on density functional theory (DFT) calculations Keith and Mankad proposed a direct bimolecular reaction that is likely unconnected to borylation catalysis.[13]

The initial steps of this borylation process are intriguing because there are several possible species that could be photoactivated during catalysis. The thermal B-H bond activation across the Fe-Cu bond leading to (IPr)Cu-H and $Cp(CO)_2$Fe-BPin mononuclear species is endothermic by more than 25 kcal/mol. This suggests that there would be a low concentration of the $Cp(CO)_2$Fe-BPin intermediate available for photoactivation, and the quantum yield of these types of metal carbonyl complexes are typically low. Alternative to photoactivation of a mononuclear intermediate, it could be possible that catalyst **1** undergoes CO photodissociation to initiate catalysis. However, this catalyst has a single Fe-Cu metal-metal bond that could fragment upon irradiation rather than CO dissociation. CO photodissociation from **1** would give the monocarbonyl intermediate (IPr)CuFeCp(CO), which could then undergo dinuclear B-H activation and subsequent arene borylation.

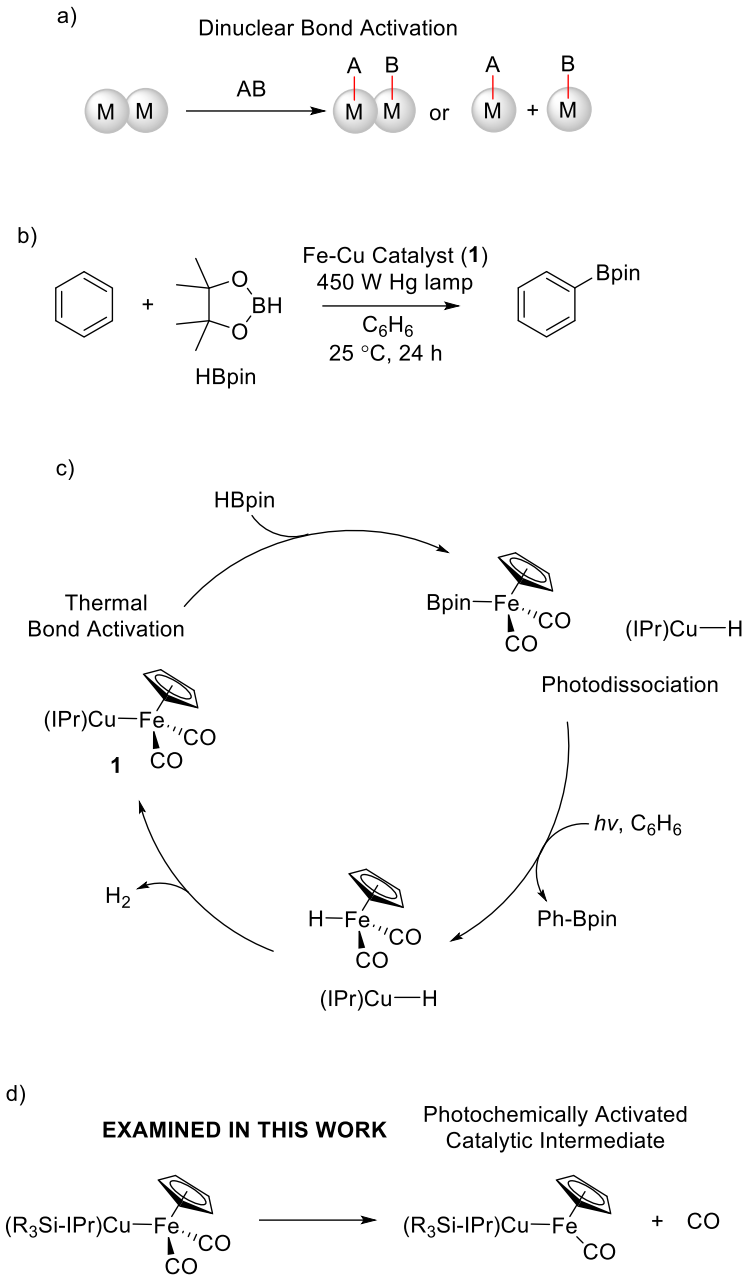

Scheme 1. a) Schematic view of bond activation reactions across a heterodinuclear metal-metal bond. b) Mankad's Fe-Cu photochemical heterodinuclear-catalyzed benzene borylation reaction.[11] c) Previously proposed catalytic cycle involving dinuclear thermal (dark) B-H bond activation, mononuclear CO photodissociation, and reformation of the Fe-Cu catalyst **1**. d) Alternative first catalytic step involving photodissociation of CO from **1** to generate a coordinatively unsaturated heterodinuclear intermediate. IPr = IPr = N,N-bis(2,6-diisopropylphenyl)imidazol-2-ylidene).

One approach to examine the feasibility of heterodinuclear CO photodissociation to initiate catalysis is to use time-resolved vibrational spectroscopy to directly detect the monocarbonyl (IPr)CuFeCp(CO) intermediate.[14] In this work we report the synthesis and X-ray characterization of a triethylsilyl-substituted Fe-Cu catalyst that provided cyclohexane solubility to conduct time-resolved UV/IR studies. We also present time-resolved vibrational spectroscopic measurements that show that photolysis of the catalysis with UV light suggests that CO photodissociation from the **1** is plausible without metal-metal bond cleavage (Scheme 1d). Overall, this provides the ability to propose a new possible catalytic cycle for photocatalytic arene borylation.

RESULTS AND DISCUSSION

To identify the initial photo-generated intermediates, time-resolved IR measurements of the CO vibrational spectrum was performed using catalyst **1**. However, initial measurements in benzene solvent showed overlap of the Fe-CO modes with vibrational modes in the solvent making identification of intermediate very difficult. Alkane solvents have no absorbances in the metal-CO region of the IR spectrum, but the dinuclear catalyst **1** is not soluble in the alkane at high enough concentrations to allow measurement of transient vibrational spectra. To address this limitation, we synthesized a silyl-substituted version of the Fe-Cu complex (**5**, Scheme 2) that provided significant solubility in cyclohexane, and the silyl-appended catalyst is competent for borylation.[11]

The synthesis of complex **5** began with protection of commercially available imidazolium ligand **2** with borane at the 2-position. Next, deprotonation of the imidazole with *n*-butyl lithium followed by quenching with chlorotriethylsilane provided silylated imidazole **3**.[15] The borane group was then removed by treatment with triflic acid and methanol and the corresponding

imidazolium salt was exposed to sodium tert-butoxide and CuCl to provide the desired copper(I) carbene complex **4**. To finish the synthesis, complex **4** was treated with anionic potassium cyclopentadienyldicarbonylferrate (KFp) to provide the final heterobimetallic complex **5** in 79% yield. X-ray quality single crystals of complex **2** were grown via vapor deposition with hexanes and toluene and the X-ray crystal structure is shown in Scheme 2b. Importantly, while the addition of the triethylsilane imparted solubility in cyclohexane, it did not significantly impact the bonding of the Fe-Cu complex. For example, the Fe–Cu distance in **5** is 2.349 Å, which is nearly identical to **1** (2.346 Å).[16]

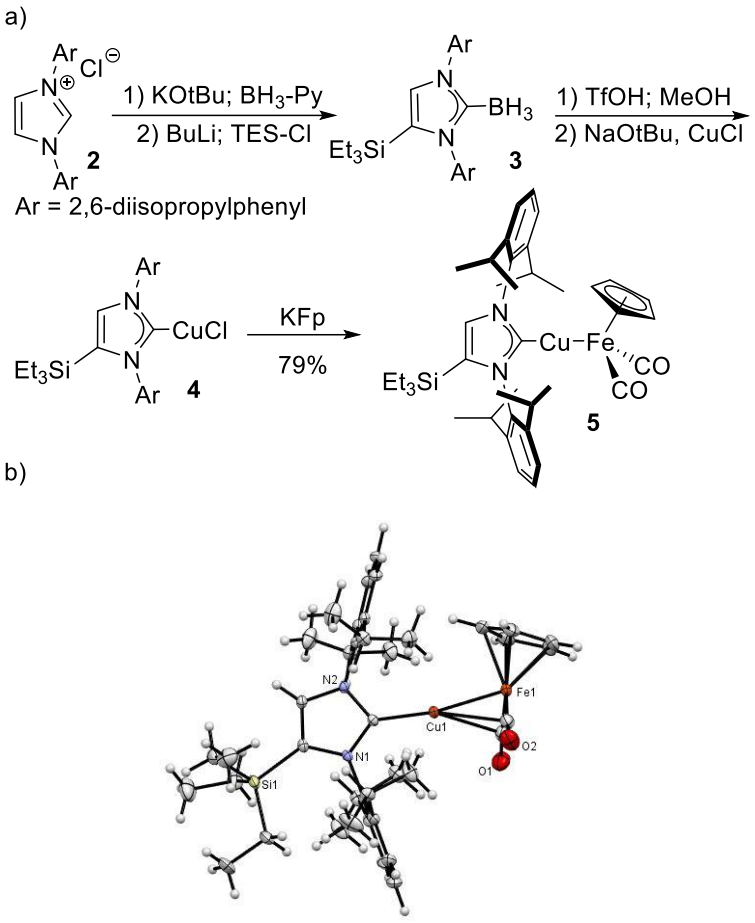

Scheme 2. a) Synthetic scheme for the triethylsilyl-substituted Fe-Cu complex **5**. b) X-ray structure of **5**.

With a cyclohexane soluble version of the Fe-Cu catalyst synthesized, we proceeded with time-resolved FTIR experiments. Alkane solutions are typically viewed as weakly coordinating solvents, but can induce caging effects.[17] Spectroscopic measurements were performed using a modified Bruker IFS-66 FTIR spectrometer in rapid scan mode for millisecond resolution, and step scan mode for microsecond resolution. The detector was a small area Mercury Cadmium Teluride, MCT, detector with a rise time of 10 ns, and an optical filter which limited the signal to the M-CO stretching region from 1400-2150 cm^{-1}. The internal 14-bit digitizer was used, yielding spectra with a resolution of 4 cm^{-1} every 5 microseconds in step-scan mode, and spectra every 14 ms in rapid scan mode. UV light for excitation was from a Continuum Powerlite 9100 YAG laser, with frequency tripling optics which yielded 9 ns pulses at 355 nm. Pulse energies were kept less than 5 mJ to minimize sample degradation, and thermal effects. This wavelength was selected because complexes **5** and **1** have broad absorption bands in the UV from 300-400 nm (see supporting information), and so the 355 nm laser light will excite the complex to the same excited electronic state as the mercury lamp used by Mankad. Samples were 3 mM in concentration, were prepared in an oxygen and water free environment, and were purged with nitrogen gas during measurement to keep them air and water free.

Figure 1 shows the IR absorption spectrum of complex **5** in the CO stretch region and the transient IR spectrum change 45 μs after UV excitation. The symmetric and anti-symmetric Fe-CO stretches of **5** occur at 1869 and 1925 cm^{-1}, and show a decrease in absorbance after excitation. In addition, a new absorption peak appears at 1888 cm^{-1} indicative of the formation of a monocarbonyl species. This suggests that UV excitation causes CO photodissociation from **5** to generate a coordinatively unsaturated (Et_3Si-IPr)CuFeCp(CO) intermediate. Consistent with these measurements, M06-L[18]/6-31G**[LANL2DZ] (chosen because of the first-row transition metals)

DFT calculations in cyclohexane solvent gave antisymmetric and symmetric CO stretches for **5** at 1857 and 1907 cm^{-1} (scaled using a 0.952 factor[19]). The calculated (Et_3Si-IPr)CuFeCp(CO) structure gave a stretch at 1824 cm^{-1}, in qualitative agreement with our measured spectra, but slightly shifted to lower frequency. Calculation of (Et_3Si-IPr)CuFeCp(CO) with a single cyclohexane within the Fe metal coordination sphere increases the CO stretch frequency to 1929 cm^{-1}, which is closer to the measured absorbance. Importantly, if UV excitation induced homolytic cleavage of the Fe-Cu bond we would expect to observe two new CO absorbances, which were not observed.

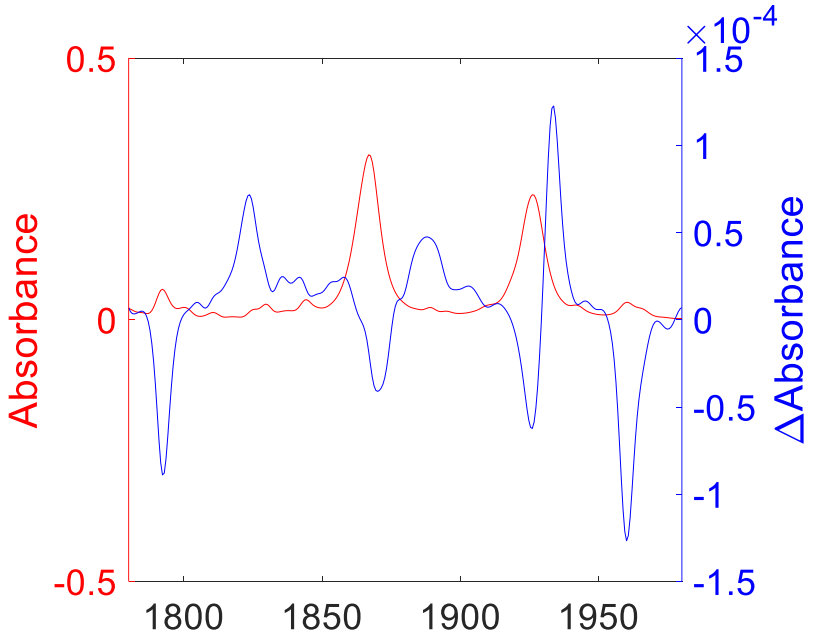

Figure 1. Static IR absorption spectrum (in cm^{-1}) of Fe-Cu complex **5** in cyclohexane solution (red) and transient IR spectrum 45 μs after UV excitation (blue).

Unfortunately, complex **5** showed a relatively low quantum yield of 4% for CO photodissociation. This is likely due internal conversion to the electronic ground state and non-radiative cooling. This somewhat complicated the IR spectrum because trace amounts of a highly

photoactive $Cp_2Fe_2(CO)_4$ led to negative bleach peaks at 1792 and 1960 cm^{-1} and new positive absorbance peaks at 1822 and 1933 cm^{-1} (Figure 1). To confirm these peaks are due to $Cp_2Fe_2(CO)_4$, Figure 2 shows the overlay of transient IR spectra of complex **5** at 45 μs after excitation and $Cp_2Fe_2(CO)_4$ 50 μs after excitation.

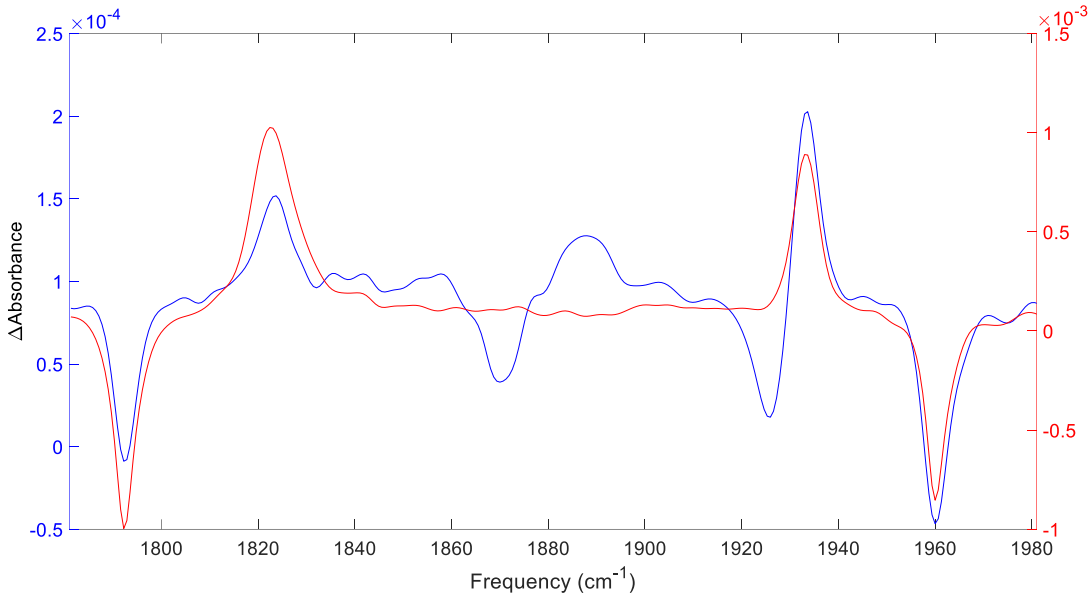

Figure 2. Transient IR spectra of complex **5** 45 µs excitation (blue) and $Cp_2Fe_2(CO)_4$ 50 µs after excitation (red).

George recently showed that after UV excitation this dimer undergoes loss of CO to form a triply bridged $Cp_2Fe_2(\mu\text{-}CO)_3$ complex that is relatively stable with a spectrum that matches our ours (see Figures 1 and 2).[20] While these peaks are small in the static IR spectrum shown in Figure 1, the quantum yield for CO dissociation for the iron dimer is >80%, and therefore small concentrations can result in large bleach and absorbance peaks in the transient spectrum. The presence of the dimer can be detected in the IR spectrum prior to UV light photolysis, which indicates that while the NMR showed no unwanted side products a minor amount of iron dimer could not be removed. Alternatively, $Cp_2Fe_2(CO)_4$ could potentially be generated from Fe-Cu bond

homolysis. Previous work has shown that metal-metal bond fragmentation is competitive with CO photodissociation.[14] For example, for $(CO)_5M\text{-}M(CO)_5$ type species there can be competition between metal-metal bond homolysis, dissociation of CO, and nondissociative relaxation,[21] and these routes are generally heavily influenced by excitation wavelength.[22] While we cannot completely rule out that a minor amount of $Cp_2Fe_2(CO)_4$ is formed under UV light exposure due to Fe-Cu metal fragmentation,[23] this is less likely since this compound is present prior to photolysis. Additionally, we do not see new $CpFe(CO)_2$ absorbances in time-resolved data (see below).

Our assignment of a dicarbonyl to monocarbonyl change upon exposure to UV light is consistent with many previous reports for mononuclear or homodinuclear complexes. For example, as a comparison to our measured values, $(acac)Rh(CO)_2$ in cyclohexane showed dicarbonyl stretches at 2082 and 2013 cm^{-1} and then the monocarbonyl showed a single stretch at 1996 cm^{-1}.[24] For this $(acac)Rh(CO)_2$ complex, the transient bleaches at the CO stretch frequencies were recovered at about 40 ps time. Also related, Lees showed that $CpRh(CO)_2$ in decalin with 313 and 458 nm light that the monocarbonyl can be trapped with triphenylphosphine.[25] For this complex the bleaching of dicarbonyl CO bands occurred at 2046 and 1982 cm^{-1} with concurrent new monocarbonyl peak at 1954 cm^{-1} for the phosphine bound structure. Harris also examined several dicarbonyl Cp-metal complexes. For example, triplet $CpCo(CO)_2$ in a heptane shows a monocarbonyl at 1990 cm^{-1} and remains for about 660 ps.[26,27] While a tricarbonyl, but related to borylation reactions, Hartwig, Webster, and Harris reported nanosecond and microsecond IR for the metal tricarbonyl $Cp^*W(CO)_3(Bpin)$. In pentane, UV-IR analysis showed bleaches at 1899, 1914, and 2000 cm^{-1}.[28] These peaks changed on the 30-200 ps time scale. In addition to these bleaches there was also peaks from W-BPin fragmentation with very fast recombination and the

growth of a Cp*W(CO)$_3$(pentane) complex, which can be seen on the nanosecond and microsecond time scales.

We next examined time-resolved changes in the IR spectrum of **5**. Figure 3 shows snapshots of the evolution of the absorbance peaks over 85 μs. At 25 μs after UV excitation the two negative peaks at 1868 and 1925 cm^{-1} have fully formed. These bleach peaks show a small recovery over 85 μs, possibly due to a small amount of CO recombination. The positive peak at 1885 cm^{-1} is completely gone by 85 μs suggesting that the monocarbonyl intermediate is unstable if it cannot form a complex with one of the reaction partners, such as HBpin or benzene. However, under catalytic conditions (Et$_3$Si-IPr)CuFeCp(CO) likely persists for substantially longer time through coordination with reaction substrates.

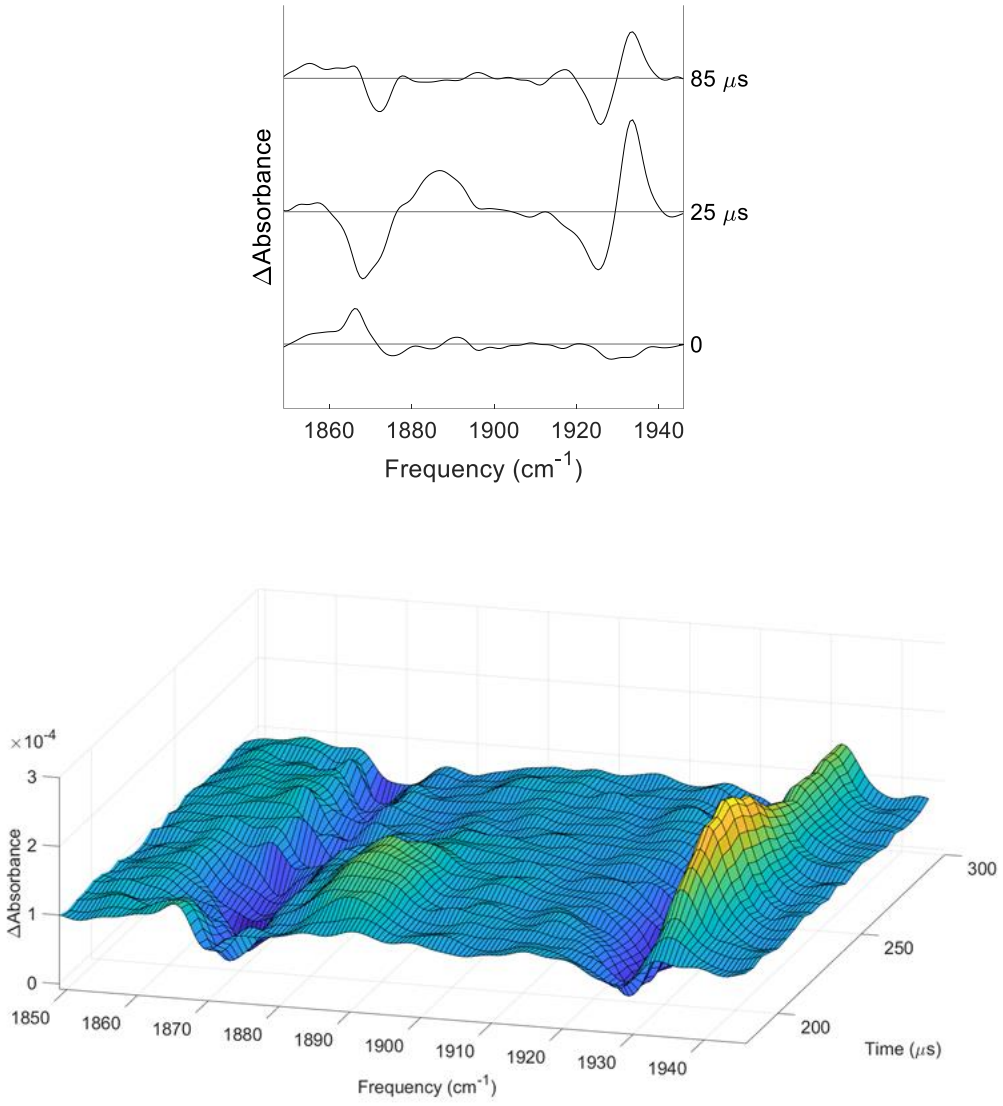

Figure 3. Top: Change in absorbance spectrum of **5** before UV laser excitation, 25 μs after excitation, and 85 μs after excitation. Bottom: Change in absorbance of complex **5** after UV excitation as a function of time.

To further distinguish between dinuclear monocarbonyl and mononuclear monocarbonyl species, we also synthesized and measured the time-resoved IR absorption spectrum of FeCp(CO)-$_2$BPin (FpBpin), which was originally proposed to be the photoactivated intermediate during arene borylation catalysis. Figure 4 shows the absorbance spectrum of the FpBpin complex in the CO stretch region, and the transient spectrum 45 μs after UV excitation. The static spectrum shows

negative absorption peaks at 1960 and 2005 cm^{-1} from Fp dimer that is also in solution, and an additional absorbance at 2012 cm^{-1} that is due to the FpBpin complex. The transient IR spectrum shows these same peaks as negative absorbances for both the Fp dimer and the FpBpin complex. Together, these spectra demonstrate that the CO stretches for the FpBpin complex are at a significantly higher frequency than those for the Fe-Cu complex and would be inconsistent with the spectra shown in Figures 1 and 2.

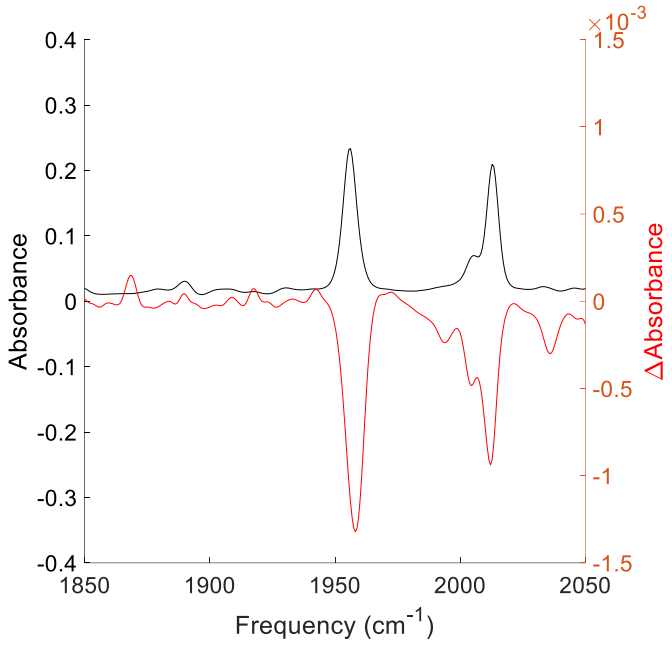

Figure 4. Static IR absorption spectrum of FpBpin complex in cyclohexane solution (black) and transient IR spectrum 45 μs after UV excitation (red).

We have also measured the transient IR spectrum for photolysis of complex **5** in cyclohexane with added HBpin. Figure 5 shows a comparison of complex **5** in cyclohexane with HBpin and the FpBpin complex. The spectrum of complex **5** with HBpin in solution shows bleach peaks at 1860 and 1925 cm^{-1} and a new absorbance peak between the bleaches, similar to the transient spectrum without HBPin in solution. The time dependance of this new absorbance

indicates that the HBpin stabilizes the monocarbonyl intermediate where it can be detected for several hundred milliseconds rather than decaying in about 80 μs without HBPin in the solution. The FpBpin complex shows no bleaches or new peaks in this region of the spectrum.

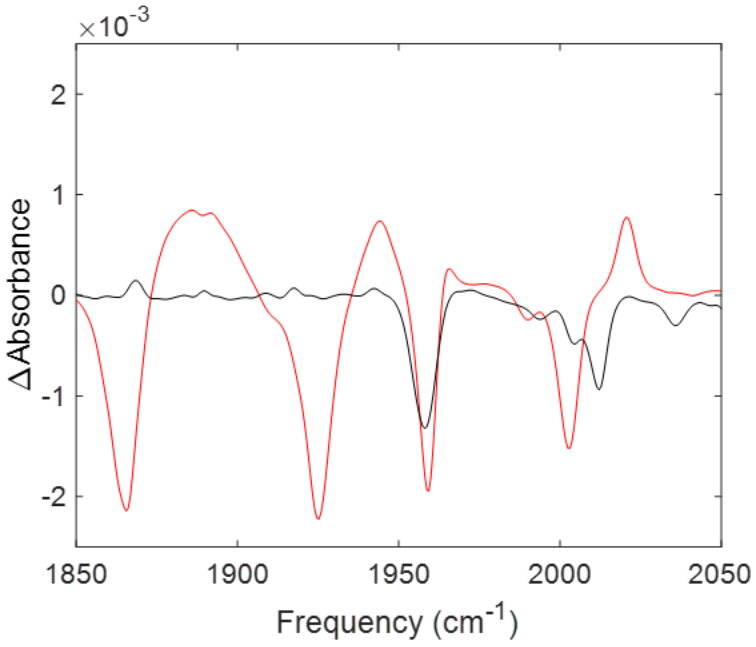

Figure 5. Transient IR spectra of complex **5** in solution with Bpin(red) 1200 milliseconds after excitation and FpBpin (black) 1200 milliseconds after excitation.

With the static and time-resolved IR information, it is now possible to propose an alternative catalytic cycle. Scheme 3 shows that UV-induced CO dissociation results in conversion of heterodinuclear **5** (or **1**) to the corresponding dinuclear monocarbonyl intermediate **6**. After **6** is formed, while not directly measured by our current studies, it is likely that this complex **6** is thermally reactive towards HBpin and can undergo B-H addition across the Fe-Cu metal-metal bond to generate (NHC)Cu-H and Cp(CO)Fe-BPin. The remainder of the catalytic cycle is similar

to Mankad and Keith's[13] proposal where the Fe-BPin complex can react with benzene to generate the Ph-Bpin and reformation of the dinuclear complex generates H_2.

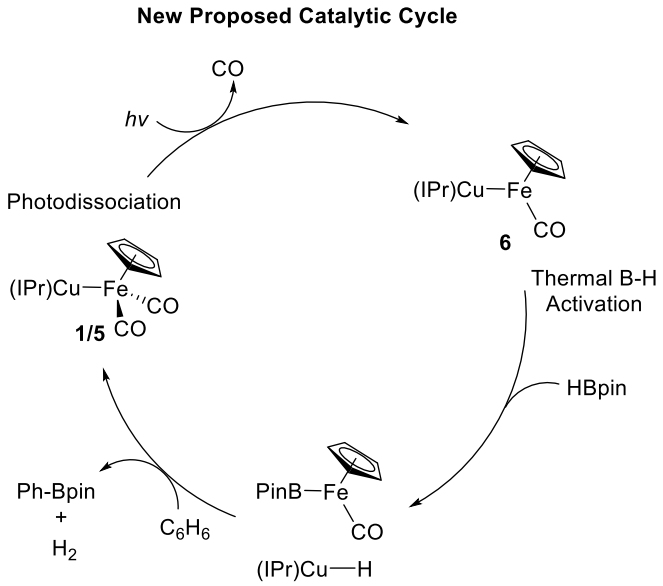

Scheme 3. Potential new catalytic cycle based on UV-IR examination of heterodinuclear complex **5**.

CONCLUSIONS

In this work we examined the possibility of photocatalysis being initialized through UV-induced CO photodissociation from an Fe-Cu heterodinuclear catalyst. To accomplish this, we synthesized a new silylated, alkane-soluble Fe-Cu complex. Static and time-resolved IR after UV laser excitation showed that the Fe-Cu metal-metal bond remains intact and that CO dissociation occurs. This suggests that catalysis begins with a CO photodissociation rather than thermal B-H bond activation. In cyclohexane the lifetime of intermediate **6** is likely on the μs time scale or less, but added HBPin likely stabilizes this coordinatively unsaturated intermediate, and we detected it at 1200 miliseconds with HBPin present in solution. However, from this work it was clear that this dinuclear complex has a very low quantum yield of photodissociation of CO and this work does

not provide direct comparison of possible rates for reaction between the dinuclear photogenerated monocarbonyl with substrates versus thermal generated mononuclear complexes and photoactivation. But it does suggest that the Fe-Cu heterodinuclear is competent for photoactivation.

ASSOCIATED CONTENT

Supporting Information. Experimental details and procedures. The Supporting Information is available free of charge on the ACS Publications website.

AUTHOR INFORMATION

Corresponding Author

*dhe@chem.byu.edu, asplund@chem.byu.edu, dmichaelis@chem.byu.edu

Conflict of Interest Statement

The authors declare no competing financial interests.

Author Contributions

J.T.D. performed UV/IR studies. E.E.M. and M.R.T. completed synthesis. K.J.C. assisted in synthesis, performed UV/IR studies, and computed vibrational frequencies. D-H.K. initiated synthesis and UV/IR studies. D.J.M. direct synthesis work, interpreted data, and edited the

manuscript. M.C.A. directed UV/IR studies, interpreted data, and edited the manuscript. D.H.E conceived of the project, directed research, interpreted data, and wrote and edited the manuscript.

Funding Sources

D.H.E. thanks the National Science Foundation Chemical Catalysis Program for support (CHE-1764194). D.J.M thanks the Chemical Synthesis Program of the National Science Foundation for support (CHE-1665015).

ACKNOWLEDGEMENT

We thank BYU Department of Chemistry and Biochemistry and College of Physical and Mathematical Sciences for facilities.

REFERENCES

1. a) Sinfelt, J. H. Bimetallic Catalysts: Discoveries, Concepts and Applications; John Wiley and Sons: New York, 1983. b) Bullock, R. M.; Casey, C. P. Heterobimetallic Compounds Linked by Heterodifunctional Ligands. *Acc. Chem. Res.* **1987**, *20*, 167-173. c) Zanello, P.; Tamburini, S.; Alessandro Vigato, P.; Antonio Mazzocchin, G. Synthesis, Structure and Electrochemical Characterization of Homo- and Heterodinuclear Copper Complexes with Compartmental Ligands. *Coord. Chem. Rev.* **1987**, *77*, 165-273. d) Stephan, D. W. Early-late Heterobimetallics. *Coord. Chem. Rev.* **1989**, *95*, 41-107. e) Beuken, E. K. van den; Feringa, B. L. Bimetallic Catalysis by Late Transition Metal Complexes. *Tetrahedron* **1998**, *54*, 12985-13011. f) Wheatley, N.; Kalck,

P. Structure and Reactivity of Early-Late Heterobimetallic Complexes. *Chem. Rev.* **1999**, *99*, 3379-3419. g) Gade, L. H. Highly Polar Metal-Metal Bonds in "Early-Late" Heterobimetallic Complexes. *Angew. Chem. Int. Ed.* **2000**, *39*, 2658-2678. h) Oro, L. A.; Sola, E. Mechanistic Aspects of Dihydrogen Activation and Catalysis by Dinuclear Complexes in *Recent Advances in Hydride Chemistry*, Elsevier, **2001**, 299-327.

2. Hostetler, M. J.; Bergman, R. G. Synthesis and Reactivity of Cp Synthesis and Reactivity of $Cp_2Ta(CH_2)_2Ir(CO)_2$: an Early-late Heterobimetallic Complex that Catalytically Hydrogenates, Isomerizes and Hydrosilates Alkenes. *J. Am. Chem. Soc.* **1990**, *112*, 8621-8623.

3. a) Gelimini, L.; Stephan, D. W. Preparation, Reactivity, Hydroformylation Catalysis, and Structural Studies of the Early Transition Metal/Late Transition Metal Heterobimetallic Complexes $Cp_2M(\mu\text{-}PR_2)_2M'H(CO)PPh_3$ (M = Zr, Hf; M' = Rh, Ir). *Organometallics*, **1988**, *7*, 849-855. b) Dickson, R. S.; De Simone, T.; Campi, E. M.; Jackson, W. R. Hydroformylation of Alkenes and Alkynes using a Heterobinuclear Rh-W Catalyst. *Inorg. Chim. Acta* **1994**, *220*, 187-192. c) Rida, M. A.; Smith, A. K. A Bimetallic Hydroformylation Catalyst: High Regioselectivity through Heterobimetallic Cooperativity. *J. Mol. Catal. A: Chem.* **2003**, *202*, 87-95.

4. a) Lindenberg, F.; Shribman, T.; Sieler, J.; Hey-Hawkins, E.; Eisen, M. Dinuclear Phosphido- and Arsenido Early/Late Transition Metal Complexes. Efficient Catalysts for Ethylene Polymerization. *J. Organomet. Chem.* **1996**, *515*, 19-25. b) Yan, X.; Chernega, A.; Green, M. L. H.; Sander, J.; Souter, J.; Ushioda, T. Homo- and Hetero-binuclear Ansa-metallocenes of the Group 4 Transition Metals as Homogeneous Co-catalysts for the Polymerization of Ethane and Propene. *J. Mol. Catal. A: Chem.* **1998**, *128*, 119-141. c) Motta, A.; Fragalà, I. L.; Marks, T. J. Proximity and Cooperativity Effects in Binuclear d Olefin Polymerization Catalysis. Theoretical Analysis of Structure and Reaction Mechanism. *J. Am. Chem. Soc.* **2009**, *131*, 3974-3984.

5. a) Ozawa, F.; Park, J. W.; Mackenzie, P. B.; Schaefer, W. P.; Henling, L. M.; Grubbs, R. H. Structure and Reactivity of Titanium-Platinum and -Palladium Heterobinuclear Complexes μ-Methylene Ligands. *J. Am. Chem. Soc.* **1989**, *111*, 1319-1327. b) Dias, E. L.; Grubbs, R. H. Synthesis and Investigation of Homo- and Heterobimetallic Ruthenium Olefin Metathesis Catalysts Exhibiting Increased Activities. *Organometallics* **1998**, *17*, 2758-2767.

6. a) Thomas, C. M. Metal-metal Multiple Bonds in Early/Late Heterobimetallic Complexes: Applications Toward Small Molecule Activation and Catalysis. *Comments on Inorganic Chemistry* **2011**, *32*, 14. b) Cooper, B. G.; Napoline, J. W.; Thomas, C. M. Catalytic Applications of Early/Late Heterobimetallic Complexes *Catal. Rev.* **2012**, *54*, 1-40.

7. a) Mankad, N. P. Selectivity Effects in Bimetallic Catalysis. *Chem. Eur. J.* **2016**, *22*, 5822-5829. b) Powers, I. G.; Uyeda, C. Metal-Metal Bonds in Catalysis. *ACS Catal.* **2017**, 7, 936-958.

8. a) Ritleng, V.; Chetcuti, M. J. Hydrocarbyl Ligand Transformations on Heterobimetallic Complexes. *Chem. Rev.* **2007**, *107*, 797-858. b) Maggini, S. Classification of P,N-binucleating Ligands for Hetero- and Homobimetallic Complexes. *Coordination Chem. Rev.* **2009**, *253*, 1793-1832. c) Vlugt, J. I. van der Cooperative Catalysis with First-Row Late Transition Metals. *Eur. J. Inorg. Chem.* **2012**, 363-375.d) Bratko, I.; Gómez, M. Polymetallic complexes linked to a single-frame ligand: cooperative effects in catalysis. *Dalton Trans.* **2013**, *42*, 10664-10681. e) Buchwalter, P.; Rose, J.; Braunstein, P. Multimetallic Catalysis Based on Heterometallic Complexes and Clusters. *Chem. Rev.* **2015**, *115*, 28-126. f) Ed. Kalck, P.; Homo- and Heterobimetallic Complexes in Catalysis: Cooperative Catalysis Topics in Organometallic Chemistry, Vol. 59, **2016**, Springer.

9. Cammarota, R. C.; Vollmer, M. V.; Xie, J.; Ye, J.; Linehan, J. C.; Burgess, S. A.; Appel, A. M.; Gagliardi, L.; Lu, C. C. A bimetallic Nickel-Gallium Complex Catalyzes CO_2 Hydrogenation via the Intermediacy of an Anionic d^{10} Nickel Hydride. *J. Am. Chem. Soc.* **2017**, *139*, 14244-14250.

10. Siedschlag, R. B.; Bernales, V.; Vogiatzis, K. D.; Planas, N.; Clouston, L. J.; Bill, E.; Gagliardi, L.; Lu, C. C. Catalytic Silylation of Dinitrogen with a Dicobalt Complex. *J. Am. Chem. Soc.* **2015**, *137*, 4638-4641.

11. a) Mazzacano, T. J.; Mankad, N. P. Base Metal Catalysts for Photochemical C–H Borylation That Utilize Metal-Metal Cooperativity. *J. Am. Chem. Soc.* **2013**, *135*, 17258-17261. b) Leon, N. J.; Yu, H.-C.; Mazzacano, T. J.; Mankad, N. P. Pursuit of C–H Borylation Reactions with Non-Precious Heterobimetallic Catalysts: Hypothesis-Driven Variations on a Design Theme. *Synlett* **2020**, *31*, 125-132.

12. Waltz, K. M.; Hartwig, J. F. Functionalization of Alkanes by Isolated Transition Metal Boryl Complexes. *J. Am. Chem. Soc.* **2000**, *122*, 11358-11369.

13. Parmelee, S. R.; Mazzacano, T. J.; Zhu, Y.; Mankad, N. A.; Keith, J. A. A Heterobimetallic Mechanism for C-H Borylation Elucidated from Experimental and Computational Data. *ACS Catal.* **2015**, *5*, 3689-3699.

14. Perutz, R. N.; Torres, O.; Viček Jr., A. Photochemistry of Metal Carbonyls. Comprehensive Inorganic Chemistry II. 229-253.

15. Solovyev, A.; Lacote, E.; Curran, D. P. Ring Lithiation and Functionalization of Imidazol-2-ylidene-boranes. *Org. Lett.* **2011**, *13*, 6042-6045.

16. Jayarathne, U.; Mazzacano, T. J.; Bagherzadeh, S.; Mankad, N. P. Heterobimetallic Complexes with Polar, Unsupported Cu–Fe and Zn–Fe Bonds Stabilized by N-Heterocyclic Carbenes. *Organometallics* **2013**, *32*, 3986-3992.

17. Yang, H.; Snee, P. T. Kotz, K.; Payne, C. K.; Harris, C. B. Femtosecond Infrared Study of the Dynamics of Solvation and Solvent Caging. *J. Am. Chem. Soc.* **2001**, *123*, 4204-4210.

18. a) Structures were optimized with the SMD cyclohexane model. Marenich, A. V.; Cramer, C. J.; Truhlar, D. G. Universal Solvation Model Based on Solute Electron Density and on a Continuum Model of the Solvent Defined by the Bulk Dielectric Constant and Atomic Surface Tensions. *J. Phys. Chem. B* **2009**, *113*, 6378-6396. b) Zhao, Y.; Truhlar, D. G. The M06 Suite of Density Functionals for Main Group Thermochemistry, Thermochemical Kinetics, Noncovalent Interactions, Excited States, and Transition Elements: Two New Functionals and Systematic Testing of Four M06-Class Functionals and 12 Other Functionals. *Theor. Chem. Acc.* **2008**, *120*, 215-241. c) Gaussian 16, Revision B.01, Frisch, M. J.; Trucks, G. W.; Schlegel, H. B.; Scuseria, G. E.; Robb, M. A.; Cheeseman, J. R.; Scalmani, G.; Barone, V.; Petersson, G. A.; Nakatsuji, H.; Li, X.; Caricato, M.; Marenich, A. V.; Bloino, J.; Janesko, B. G.; Gomperts, R.; Mennucci, B.; Hratchian, H. P.; Ortiz, J. V.; Izmaylov, A. F.; Sonnenberg, J. L.; Williams-Young, D.; Ding, F.; Lipparini, F.; Egidi, F.; Goings, J.; Peng, B.; Petrone, A.; Henderson, T.; Ranasinghe, D.; Zakrzewski, V. G.; Gao, J.; Rega, N.; Zheng, G.; Liang, W.; Hada, M.; Ehara, M.; Toyota, K.; Fukuda, R.; Hasegawa, J.; Ishida, M.; Nakajima, T.; Honda, Y.; Kitao, O.; Nakai, H.; Vreven, T.; Throssell, K.; Montgomery, J. A., Jr.; Peralta, J. E.; Ogliaro, F.; Bearpark, M. J.; Heyd, J. J.; Brothers, E. N.; Kudin, K. N.; Staroverov, V. N.; Keith, T. A.; Kobayashi, R.; Normand, J.; Raghavachari, K.; Rendell, A. P.; Burant, J. C.; Iyengar, S. S.; Tomasi, J.; Cossi, M.; Millam, J. M.; Klene, M.; Adamo, C.; Cammi, R.; Ochterski, J. W.; Martin, R. L.; Morokuma, K.; Farkas, O.; Foresman, J. B.; Fox, D. J. Gaussian, Inc., Wallingford CT, 2016.

19. Kanchanakungwankul, S.; Bao, J. L.; Zheng, J.; Alecu, I. M.; Lynch, B. J.; Zhao, Y.; Truhlar D. G. Database of Frequency Scale Factors for Electronic Model Chemistries – Version 4. https://comp.chem.umn.edu/freqscale/. Accessed 1/1/2021.

20. a) Brookes, C. M.; Lomont, J. P.; Nguyen, S. C.; Calladine, J. A.; Sun, X. Z.; Harris, C. B.; George, M. W. New insights into the photochemistry of $[CpFe(CO)_2]_2$ using picosecond through microsecond time-resolved infrared spectroscopy (TRIR). *Polyhedron* **2014**, *72*, 130-134. b) George, M. W.; Dougherty, T. P.; Heilweil, E. J. UV Photochemistry of $[CpFe(CO)_2]_2$ (Cp = η^5-C_5H_5) Studied by Picosecond Time-Resolved Infrared Spectroscopy. *J. Phys. Chem.* **1996**, *100*, 201–206.

21. a) Meyer, T. J.; Caspar, J. V. Photochemistry of metal-metal bonds. *Chem. Rev.* **1985**, *85*, 187-218. b) Wrighton, M.; Bredesen, D. Symmetrical cleavage of the metal-metal bond in decacarbonyldirhenium (0) by ultraviolet irradiation. *J. Organomet. Chem.* **1973**, *50*, C35-C38. c) Wegman, R. W.; Olsen, R. J.; Gard, D. R.; Faulkner, L. R.; Brown, T. L. Flash photolysis study of the metal-metal bond homolysis in dimanganese decacarbonyl and dirhenium decacarbonyl. *J. Am. Chem. Soc.* **1981**, *103*, 6089-6092. d) Firth, S.; Hodges, P. M.; Poliakoff, M.; Turner, J. J.; Therien, M. J. Selective loss of CO in the photochemistry of $MnRe(CO)_{10}$: a study using matrix isolation and time-resolved infrared spectroscopyl. *J. Organomet. Chem.* **1987**, *331*, 347-355.

22. a) Wrighton, M. S.; Ginley, D. S. Photochemistry of metal-metal bonded complexes. II. Photochemistry of rhenium and manganese carbonyl complexes containing a metal-metal bond. *J. Am. Chem. Soc.* **1975**, *97*, 2065-2072. b) Gard, D. R.; Brown, T. L. Photochemical reactions of dirhenium decacarbonyl with water. *J. Am. Chem. Soc.* **1982**, *104*, 6340-6347. c) Kobayashi, T.; Ohtani, H.; Noda, H.; Teratani, S.; Yamazaki, H.; Yasufuku, K. Excitation wavelength dependence of photodissociation and the secondary laser pulse photolysis of dimanganese decacarbonyl.

Organometallics **1986**, *5*, 110-113. d) Seder, T. A.; Church, S. P.; Weitz, E. Photodissociation pathways and recombination kinetics for gas-phase dimanganese decacarbonyl. *J. Am. Chem. Soc.* **1986**, *108*, 7518-7524.

23. Boulanger, S. A.; Zhu, L.; Tang, L.; Saha, S.; Keszler, D. A.; Fang, C. Photoinduced Charge Transfer and Bimetallic Bond Dissociation of a Bi–W Complex in Solution. *J. Phys. Chem. Lett.* **2020**, *11*, 7575-7582.

24. Dougherty, T. P.; Grubbs, W. T.; Heilweil, E. J. Photochemistry of $Rh(CO)_2$(acetylacetonate) and related metal dicarbonyls studied by ultrafast infrared spectroscopy. *J. Phys. Chem.* **1994**, *98*, 9396-9399.

25. Drolet, D. P.; Less, A. J. Solution photochemistry of (η^5-C_5R_5)$Rh(CO)_2$ (R= H, Me) complexes: pathways for photosubstitution and C-H/Si-H bond activation reactions. *J. Am. Chem. Soc.* **1992**, *114*, 4186-4194.

26. Snee, P. T.; Payne, C. K.; Kotz, K. T.; Yang, H.; Harris, C. B. Triplet organometallic reactivity under ambient conditions: an ultrafast UV pump/IR probe study. *J. Am. Chem. Soc.* **2001**, *123*, 2255-2264.

27. Lomont, J. P.; Nguyen, S. C.; Schlegel, J. P.; Zoerb, M. C.; Hill, A. D.; Harris, C. B. Ultrafast observation of a solvent dependent spin state equilibrium in CpCo (CO). *J. Am. Chem. Soc.* **2012**, *134*, 3120-3126.

28. Sawyer, K. R.; Cahoon, J. F. Schanoski, J. E.; Glascoe, E. A.; Kling, M. F.; Schlegel, J. P.; Zoerb, M. C.; Hapke, M.; Hartwig, J. F.; Webster, C. E.; Harris, C. B. Time-resolved IR Studies on the Mechanism for the Functionalization of Primary C−H Bonds by Photoactivated Cp*$W(CO)_3$(Bpin). *J. Am. Chem. Soc.* **2010**, *132*, 1848-1859.

TOC Graphic

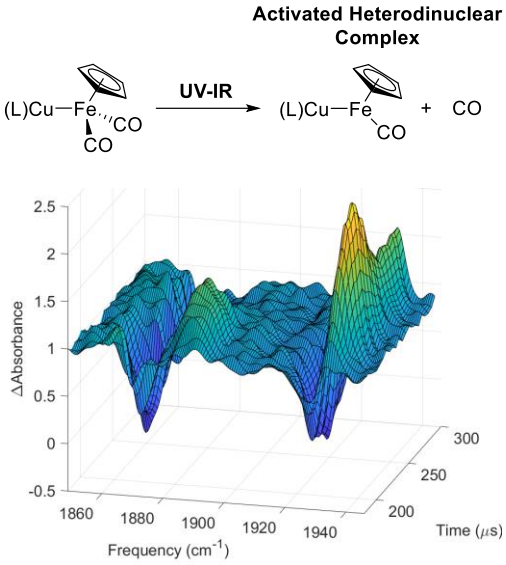
Activated Heterodinuclear Complex
(L)Cu—Fe
CO
CO
UV-IR
(L)Cu—Fe
CO
+ CO
ΔAbsorbance
2.5
2
1.5
1
0.5
0
-0.5
1860
1880
1900
1920
1940
Frequency (cm-1)
300
250
200
Time (μs)